

Differential Expression and Interaction with the Visual G-protein Transducin of Centrin Isoforms in Mammalian Photoreceptor Cells*

Received for publication, June 17, 2004, and in revised form, August 13, 2004
Published, JBC Papers in Press, August 30, 2004, DOI 10.1074/jbc.M406770200

Andreas Giessl^{‡§}, Alexander Pulvermüller^{¶§||}, Philipp Trojan[‡], Jung Hee Park[¶],
Hui-Woog Choe^{¶**}, Oliver Peter Ernst[¶], Klaus Peter Hofmann[¶], and Uwe Wolfrum^{‡ ††}

From the [‡]Institut für Zoologie, Johannes Gutenberg-Universität Mainz, 55099 Mainz, Germany, the [¶]Institut für Medizinische Physik und Biophysik, Charité-Universitätsmedizin Berlin, Schumannstrasse 20-21, 10098 Berlin, Germany, and the ^{**}Department of Chemistry, College of Natural Science, Chonbuk National University, Chonju 561-756, South Korea

Photoisomerization of rhodopsin activates a heterotrimeric G-protein cascade leading to closure of cGMP-gated channels and hyperpolarization of photoreceptor cells. Massive translocation of the visual G-protein transducin, G_t , between subcellular compartments contributes to long term adaptation of photoreceptor cells. Ca^{2+} -triggered assembly of a centrin-transducin complex in the connecting cilium of photoreceptor cells may regulate these transducin translocations. Here we demonstrate expression of all four known, closely related centrin isoforms in the mammalian retina. Interaction assays revealed binding potential of the four centrin isoforms to $G_t\beta\gamma$ heterodimers. High affinity binding to $G_t\beta\gamma$ and subcellular localization of the centrin isoforms Cen1 and Cen2 in the connecting cilium indicated that these isoforms contribute to the centrin-transducin complex and potentially participate in the regulation of transducin translocation through the photoreceptor cilium. Binding of Cen2 and Cen4 to $G\beta\gamma$ of non-visual G-proteins may additionally regulate G-proteins involved in centrosome and basal body functions.

Vertebrate rod and cone photoreceptor cells are highly polarized neurons that consist of morphologically and functionally distinct cellular compartments. Light-sensitive outer segments are linked via a non-motile connecting cilium with inner segments that contain the organelles typical for the metabolism of eukaryotic cells (see Fig. 6A). The outer segments are characterized by specialized disklike membranes where one of the best studied examples of a G-protein transduction cascade is arranged (1, 2). Photoexcitation leads to photoisomerization of the visual pigment rhodopsin (Rh^*),¹ which catalyzes GDP/

GTP exchange on the heterotrimeric holo G-protein transducin (G_t holo). This releases the α -subunit of transducin ($G_t\alpha$), which in turn activates a phosphodiesterase, catalyzing cGMP hydrolysis in the cytoplasm and closure of cGMP-gated channels localized in the plasma membrane (2, 3). The closure of these channels leads to a drop of the circulating cationic current, resulting in the hyperpolarization of the cell membrane (4). The recovery phase of the enzymatic machinery of visual transduction and rapid light adaptation of photoreceptor cells (time scale of subseconds) rely on a feedback mechanism. This depends on changes in the intracellular Ca^{2+} concentration [Ca^{2+}], affecting the phototransduction cascade through Ca^{2+} -binding proteins (5). However, massive bidirectional translocation of transduction cascade components between the functional compartments of photoreceptor cells can also contribute to a much slower adaptation of rod photoreceptor cells (6, 7).

Light-induced exchanges of signal cascade components were first noted about a decade ago (8–10) and are currently of prominent interest in the field (e.g. Hardie (11), and see current review by Giessl *et al.* (12)): upon illumination, 80% of $G_t\alpha$ and $G_t\beta\gamma$ move in minutes from the outer segment to the inner segment and the cell body of rod photoreceptor cells. A recent study indicates that binding of the photoreceptor-specific protein phosducin to $G_t\beta\gamma$ is not essential for this movement but facilitates light-driven $G_t\beta\gamma$ translocation to the inner segment (7). The G-protein subunits return to the outer segments in the dark in a more leisurely time course of hours. In contrast, arrestin translocates under these light conditions in an exactly reciprocal way (8, 10). Since any intracellular exchange between the inner and outer segmental compartments of photoreceptor cells should occur through the slender non-motile connecting cilium (13), this represents a suitable domain for potential regulation of intersegmental molecular exchange (14). Our initial studies revealed that transducin is translocated through the photoreceptor connecting cilium and further indicated that the Ca^{2+} -induced assembly of a protein-protein complex of the G-protein transducin and the cytoskeletal protein centrin 1 regulates ciliary G-protein translocation (12, 15, 16). The assembly of this centrin 1-G-protein complex strictly depends on Ca^{2+} and is mediated by the $G_t\beta\gamma$ complex.

Centrin 1 is a member of the centrin protein family, a subfamily of the parvalbumin superfamily of Ca^{2+} -binding proteins (17, 18). Centrins were first described in unicellular green

* This work was supported by Grants Ho832/6 (to A. P., O. P. E., and K. P. H.) and Wo548/3 (to U. W.) from the Deutsche Forschungsgemeinschaft (DFG) priority program SPP 1025 "Molecular Sensory Physiology" and by a grant from the FAUN-Stiftung, Nürnberg, Germany (to U. W.). The costs of publication of this article were defrayed in part by the payment of page charges. This article must therefore be hereby marked "advertisement" in accordance with 18 U.S.C. Section 1734 solely to indicate this fact.

§ Both authors contributed equally to this work.

|| To whom correspondence may be addressed: Inst. für Medizinische Physik und Biophysik, Charité-Universitätsmedizin Berlin, Ziegelstrasse 5-9, D-10117 Berlin, Germany. Tel.: 49-30-450-524176; Fax: 49-30-450-524952; E-mail: alexander.pulvermueller@charite.de.

†† To whom correspondence may be addressed: Inst. für Zoologie, Abt.1, Johannes Gutenberg-Universität Mainz, Müllerweg 6, D-55099 Mainz, Germany. Tel.: 49-6131-39-25148; Fax: 49-6131-39-23815; E-mail: wolfrum@mail.uni-mainz.de.

¹ The abbreviations used are: Rh, rhodopsin; Rh^* , photoactivated rhodopsin; G_t , retinal G-protein, transducin; MmCen1–4, mouse cen-

trin isoforms 1–4; Cen1–4, centrin isoforms 1–4; Cen1p–4p, centrin isoform 1–4 proteins; pMmC1–4: polyclonal antibody against mouse centrins 1–4; BTP, 1,3-bis[tris(hydroxymethyl)methylamino]propane; GST, glutathione S-transferase; RT, reverse transcription; $GTP\gamma S$, guanosine 5'-3-O-(thio)triphosphate; CHAPS, 3-[(3-cholamidopropyl)-dimethylammonio]-1-propanesulfonic acid.

algae where they form filamentous structures that contract in response to an increase of $[Ca^{2+}]_i$ (17–19). In vertebrates, centrin are ubiquitously expressed and commonly associated with centrosome-related structures such as spindle poles of dividing cells or centrioles in centrosomes and basal bodies (17, 18). At least four different centrin genes are expressed in mammals (20–27). As a consequence of the isoform diversity in the mammalian genome, the four mammalian centrin should exhibit differences in their subcellular localization as well as in their cellular function. Little is known about the specific subcellular localization of the different centrin isoforms in diverse cell types and tissues. Most studies on the localization of centrin in mammalian cells and tissues have been performed with polyclonal and monoclonal antibodies raised against green algae centrin that do not discriminate between the mammalian centrin isoforms. Using these antibodies, centrin were detected in the centrioles of centrosomes and in the pericentriolar matrix (28–30). In previous studies on the mammalian retina, centrin were localized in two basically distinct subcellular domains (12, 14, 16). As in other animal cells, centrin are components of centrosomes and basal bodies in retinal neurons but were also found to be present in the connecting cilium of photoreceptor cells (14–16, 32). Although our recent studies provided evidence that isoform Cen1 is localized in the connecting cilium, a ciliary expression of other centrin isoforms remained elusive (16).

Here we show by glutathione *S*-transferase (GST) pull-down assays, size exclusion chromatography, and kinetic light-scattering experiments that all four centrin isoforms bind to the $G_t\beta\gamma$ complex with different affinities. In the present study, we also demonstrated retinal expression of the four centrin isoforms. Furthermore we were able to show for the first time that the centrin are co-expressed in the same cell type, particularly in highly specialized photoreceptor cells. Nevertheless there they are localized in different subcellular domains. The localization of the centrin isoforms Cen1 to Cen3 in the photoreceptor connecting cilium suggests that these centrin can be part of the centrin-transducin complex. In contrast, the centriolar localization of centrin isoforms 2–4 indicates an additional function of these centrin isoforms.

EXPERIMENTAL PROCEDURES

Animals and Tissue Preparation—All experiments described herein conform to the statement by the Association for Research in Vision and Ophthalmology as to the care and use of animals in research. Adult Sprague-Dawley albino rats and C57BL/7 mice were maintained on a 12/12-h light/dark cycle with lights on at 6 a.m. with food and water *ad libitum*. After sacrifice of the animals in CO_2 , retinas were removed through a slit in the cornea prior to fixation and embedding for microscopy or further molecular biological and biochemical analysis. Bovine eyes were obtained from the local slaughter houses and were kept on ice in the dark until further processing.

Antibodies—Affinity-purified polyclonal rabbit antibodies against the α - and β -subunit of G-proteins were obtained from Biomol Research Laboratories, Inc. (Plymouth Meeting, PA), and a second affinity-purified polyclonal rabbit antibody against the β -subunit of G-proteins (T-20) was purchased from Molecular Probes (Eugene, OR). Monoclonal antibody against centrin (clone 20H5) and a monoclonal antibody against HsCen2p (clone hCen2.4) have been characterized previously (30, 33). Polyclonal antisera from rabbit or goat against recombinantly expressed mouse centrin 1–4 (MmCen1 to MmCen4) were generated and affinity-purified on high trap *N*-hydroxysuccinimide columns (Amersham Biosciences).

SDS-PAGE and Western Blot—For Western blots, isolated retinas or GST pull-down complexes were homogenized and placed in SDS-PAGE sample buffer (62.5 mM Tris-HCl (pH 6.8) containing 10% glycerol, 2% SDS, 5% mercaptoethanol, 1 mM EDTA, and 0.025% bromophenol blue). Proteins were separated by SDS-PAGE (34) using 15% polyacrylamide gels, transferred electrophoretically to polyvinylidene difluoride membranes (Bio-Rad), and probed with primary and secondary antibodies (32).

Recombinant Expression of Centrin Isoforms—Cloning of a mouse centrin 1 cDNA into the pGEX-4T3 expression vector (Amersham Biosciences) was described previously by Pulvermüller *et al.* (15). Mouse centrin 2, 3, and 4 cDNAs were cloned from reverse transcription (RT)-PCR products into the pGEX-4T3 expression vector (Amersham Biosciences) using BamHI and XhoI restriction sites. Expression and purification of the GST fusion protein was performed according to the manufacturer's instructions (Amersham Biosciences). After cleavage of the fusion protein with thrombin on the column, centrin was eluted in 20 mM BTP (pH 7.5) containing 130 mM NaCl and 1 mM $MgCl_2$ and passed over a benzamidine-Sepharose 6B (Amersham Biosciences) column to remove thrombin.

Membrane and Protein Preparations—Rod outer segments were prepared from frozen bovine retinas using a sucrose gradient procedure as described previously (35). Hypotonically stripped disk membranes were prepared from rod outer segments by the Ficoll floating procedure similar to the procedure described previously (36) except that 2% (w/v) Ficoll instead of 5% was used. This method yielded osmotically intact disk vesicles with a vesicle size >400 nm. Contamination by vesicle aggregates was removed by a 2- μ m filter (Roth, Karlsruhe, Germany). Membranes were either kept on ice and used within 4 days without any loss of activity or stored at $-80^\circ C$ until use. Rhodopsin concentration was determined from its absorption spectrum using $\epsilon_{500} = 40,000 M^{-1} cm^{-1}$. Transducin (G_t holo) was isolated from frozen dark-adapted bovine retinas according to Ref. 3. Subunits were further purified on Blue Sepharose (1 ml of HiTrap Blue, Amersham Biosciences) using a salt gradient (15). G_t holo, $G_t\alpha$, and $G_t\beta\gamma$ concentrations were determined by the Bradford assay (37) using bovine serum albumin as the standard. The amount of intact, activable $G_t\alpha$ was determined precisely by fluorometric titration with GTP γ S (38).

GST-Centrin Pull-down Assay—Bacteria expressing GST-centrin fusion proteins were resuspended in PBS (140 mM NaCl, 2.7 mM KCl, 10 mM Na_2HPO_4 , 1.8 mM KH_2PO_4 (pH 7.3)). Cells were lysed by lysozyme (0.2 mg/ml) and sonicated. Cleared lysates were incubated for 2 h at $4^\circ C$ with 50 μ l of glutathione-*S*-Sepharose 4B (Amersham Biosciences) in NETN buffer (20 mM Tris-HCl (pH 8.0), 100 mM NaCl, 1 mM EDTA, 0.5% Nonidet P-40) in a final volume of 500 μ l. Sepharose beads with fusion proteins were washed with NETN buffer and buffer F (20 mM Na-Hepes (pH 8.0), 2 mM EDTA, 10 mM $CaCl_2$, 100 mM NaCl, 11 mM CHAPS, 1 mM dithiothreitol) and incubated with retina extracts in buffer F for 2 h at $4^\circ C$ (final volume, 600 μ l). Beads were washed three times with buffer F, and proteins were eluted from the beads by incubation for 20–30 min at $25^\circ C$ in 50 mM Tris-HCl (pH 8.0) containing 15 mM glutathione and 11 mM CHAPS.

Size Exclusion Chromatography—Size exclusion chromatography is a very useful tool to determine protein-protein interaction (15, 39) and was used in this study to characterize direct complex formation between the four different mouse centrin (MmCen1 to MmCen4), transducin (G_t), and its subunits. To determine the binding of the centrin to transducin the molecular weight shift of the complex was used. 10 μ g of each recombinant centrin isoform and 10 μ g of G_t holo (or G_t subunits $G_t\alpha$ and $G_t\beta\gamma$) were incubated in 50 mM BTP (pH 7.0) containing 80 mM NaCl, 1 mM $MgCl_2$, and either 100 μ M $CaCl_2$ or 1 mM EGTA for 5 min at room temperature. As controls, all samples (MmCen1 to MmCen4, G_t , and G_t subunits) were incubated alone. The reaction mixtures were loaded on a SuperoseTM 12 column (Amersham Biosciences) equilibrated with the same buffer using the Smart System (Amersham Biosciences; flow rate, 40 μ l/min). Elution was monitored by absorbance at 280 nm, and 40- μ l fractions were collected for the subsequent SDS-PAGE analysis.

Kinetic Light Scattering—The gain or loss of membrane-bound protein mass can be readily measured by light-scattering changes using a setup described in detail in Heck *et al.* (40). All measurements were performed in 10-mm path cuvettes with 300- μ l volumes in 50 mM BTP (pH 7.5) containing 80 mM NaCl, 5 mM $MgCl_2$, and either 100 μ M $CaCl_2$ or 1 mM EGTA at $20^\circ C$ (15). Reactions were triggered by flash photolysis of rhodopsin with a green (500 ± 20 nm) flash attenuated by appropriate neutral density filters. The flash intensity was quantified photometrically by the amount of rhodopsin bleached and expressed in the mole fraction of photoexcited rhodopsin ($Rh^*/Rh = 32\%$). The scattering signal is interpreted as a gain of protein mass bound to disk membranes and quantified as described previously (40, 41). Light-scattering binding signals were corrected by a reference signal (N-signal) measured on a sample without added G_t holo as described previously (42).

RT-PCR—Total RNA was isolated from mouse and rat retinas using TRIzol reagent (Invitrogen). Samples of purified total RNA were treated with DNase I (Sigma) for 15 min to remove genetic DNA. To stop the

reaction the samples were treated for 15 min at 75 °C. Poly(dT)-primed cDNA synthesis (reverse transcriptase reaction) was performed using the Invitrogen cDNA Cycle™ kit and 5 µg of total RNA according to the directions. In control preparations, total RNA (DNase-treated or -untreated) was amplified by PCR without prior reverse transcriptase reactions using the MmCen1 primers. PCR was performed in a volume of 50 µl using 2.5 µl of prepared cDNA according to directions and 0.25 µg of each primer/reaction. Cycling conditions were 39 cycles at 94 °C for 1 min, 59 °C for 30 s, and 72 °C for 3 min followed by a 10-min 72 °C extension. PCR product lengths were determined on 0.8% agarose gels. As DNA markers, a 1-kb DNA ladder (Invitrogen) was used. Sequencing of PCR products was performed by Genterprise (Mainz, Germany). For sequence comparisons and oligonucleotide generation the computer program Omega™ Version 2.0 (Oxford Molecular Ltd., Oxford, UK) was used.

PCR Primers Used for RT-PCR and DNA Sequencing—Primers specific for mouse centrin isoforms were as follows: MmCen1 primers, the forward primer MmCen1-forw (5'-GTACGGATC CATGGCGTCCACC-TTCAGGAAG-3') and the reverse primer MmCen1-EF3,4-rev (5'-GC-GGCTCGAGTTAATCTTCTCGGCCATCTT-3'); MmCen2 primers, the forward primer MmCen2-EF1,2-forw (5'-GTACGGATCCACTAAAGA-AGAAATCCTGAAA-3') and the reverse primer MmCen2-rev (5'-GCG-GCTCGAGTTACAGACAAGCTGTGACCGT-3'); MmCen3 primers: the forward primer MmCen3-forw (5'-GTACGGAT CCGAGAACTGTCTG-AGGAACAGA-3') and the reverse primer MmCen3-rev (5'-GCGG CT-CGAGTATGTCACCAAGTCATAATAGC-3'); MmCen4 primers, the forward MmCen4-Nterm-forw (5'-GTACGGATCCCAAGAAGTTCGGG-AAGCCTTT-3') and the reverse primer MmCen4-rev (5'-GCG-GCTCGAGCTAATAAAGGCTGGTCTTCTT-3').

Peptide Preabsorption of pMmC Centrin Antibodies with Recombinant Expressed Centrins—To increase antibody specificity, the polyclonal antibodies pMmC1 to pMmC4 were preincubated with the appropriate recombinant centrin isoform proteins. For this purpose centrin isoform proteins were immobilized on polyvinylidene difluoride membranes (Bio-Rad) and incubated with the affinity-purified antibodies for 12 h at 4 °C in blocking solution (0.5% cold-water fish gelatin (Sigma) plus 0.1% ovalbumin (Sigma) in PBS). The following protein amounts were used: pMmC1: 200 µg of MmCen2, 350 µg of MmCen3, and 150 µg of MmCen4; pMmC2: 400 µg of MmCen1, 300 µg of MmCen3, and 200 µg of MmCen4; pMmC3: 100 µg of MmCen1 and 30 µg of MmCen4; pMmC4: 300 µg of MmCen1, 200 µg of MmCen2, and 400 µg of MmCen3. The supernatants containing the “preabsorbed” antibodies were subsequently used in Western blots or immunocytochemical experiments, respectively.

Fluorescence Staining of Retinal Cryosections—Immunofluorescence studies were essentially performed as described previously (15, 43). Briefly eyes from adult mice were prefixed in 4% paraformaldehyde in PBS for 1 h at room temperature, washed, soaked with 30% sucrose in PBS overnight, and cryofixed in melting isopentane. Cryosections were placed on poly-L-lysine-precoated coverslips (44, 45). Specimens were incubated with 50 mM NH₄Cl and 0.1% Tween 20 in PBS and blocked with blocking solution (0.5% cold-water fish gelatin (Sigma) plus 0.1% ovalbumin (Sigma) in PBS). The sections were incubated with antibodies or, in the case of double labeling, with a mixture of antibodies in blocking solution overnight at 4 °C. The specimens were washed and subsequently incubated with secondary antibodies conjugated to Alexa® 488 or Alexa 546 (Molecular Probes) in blocking solution for 1 h at room temperature in the dark. Washed sections were mounted in Mowiol 4.88 (Hoechst, Frankfurt, Germany) containing 2% *n*-propyl gallate and, in the case of triple staining, 1 µg/ml 4,6-diamidino-2-phenylindole. Mounted retinal sections were examined with a Leica DMRP microscope. Images were obtained with a Hamamatsu Orca ER CCD camera (Hamamatsu City, Japan) and processed with Adobe Photoshop (Adobe Systems, San Jose, CA).

Immunoelectron Microscopy—After 12-h dark or light adaptation, respectively, isolated rat or mouse retinas were fixed, embedded in LR White resin, and further processed for immunoelectron microscopy as described previously (45). Nanogold™ labeling (Nanoprobes, Yaphank, NY) was silver-enhanced according to Ref. 46. Counterstained sections were analyzed in an FEI Tecnai 12 Biotwin electron microscope.

RESULTS

Assembly of Transducin-Centrin Complexes—In the search for centrin 1-interacting proteins in photoreceptor cells, we have previously identified the βγ subunit of the visual G-protein transducin as a potent interacting partner for MmCen1 (15, 16). Nevertheless previous studies demonstrated the pres-

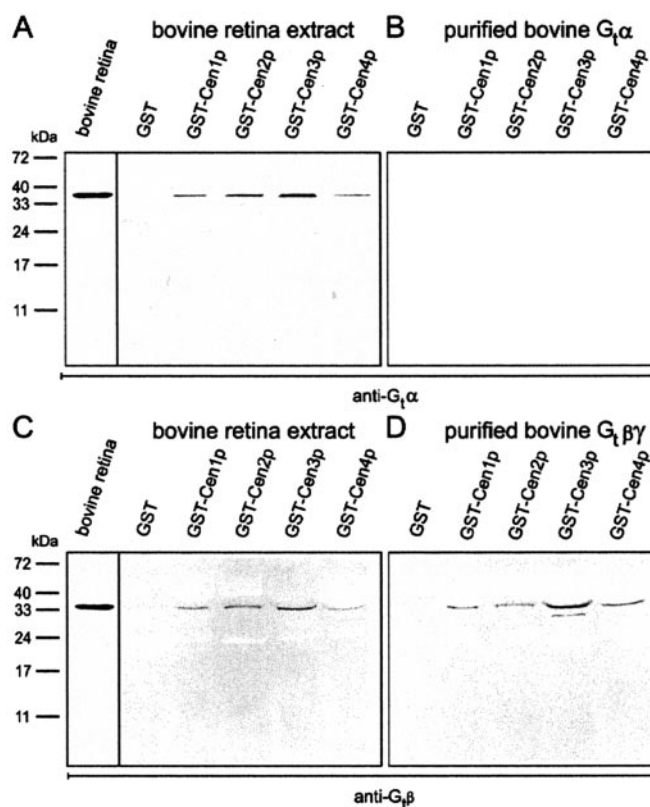


FIG. 1. GST-centrin pull-downs of transducin. GST fusion proteins were incubated with bovine retina extracts (A and C) or biochemically purified subunits of transducin, G_tα or G_tβγ, respectively (B and D). Western blot analysis with anti-G_tα (A and B) or anti-G_tβ antibodies (C and D) is shown. In bovine retina extracts the antibodies detected bands specific for the G-protein subunits (*first lanes* in A and C). None of the transducin subunits were pulled down by GST alone. All GST-centrins pulled down G_tα from bovine retina extract but not the purified bovine G_tα (A and B). All GST-centrins pulled down G_tβ from either retina extracts or purified G_tβγ heterodimers (A and C). These results indicated that all four centrin isoforms bind to heterotrimeric G_tholo via G_tβγ.

ence of four distinct centrin isogenes in mammalian genomes (12, 16). Here we addressed whether the Ca²⁺-dependent assembly of a centrin-transducin complex is restricted to the centrin isoform 1 or whether this protein-protein interaction also occurs between transducin and other centrin isoforms. To prove these interactions, we applied several independent but complementary assays.

GST-Centrin Pull-down Assays—In a first set of experiments, we tested the binding of the centrin isoforms to transducin in GST pull-down assays. For this purpose immobilized GST-tagged centrin isoforms from mouse were incubated with detergent extracts from bovine retinas. GST-centrin constructs and bound proteins were eluted from the glutathione-Sepharose beads, and transducin was detected by immunoblotting with antibodies against G_tα and G_tβ. Native transducin (G_tholo) present in retinal lysates specifically bound to GST fusion proteins of all four centrin isoforms but not to GST alone (Fig. 1A). To identify the transducin subunit that interacts with the centrins, GST-centrin constructs were added to G_tα and G_tβγ, respectively, purified from bovine photoreceptor outer segments. Western blot analyses of the GST-centrin co-precipitations with antibodies against G_tα or G_tβ, respectively, revealed that the undissociable G_tβγ was present in all co-precipitations, while G_tα was not found in any of the reactions (Fig. 1B). This demonstrated that all centrin isoforms interact with the G_tβγ as an isolated heterodimer or with G_tβγ within the heterotrimer of transducin (G_tholo = G_tαβγ).

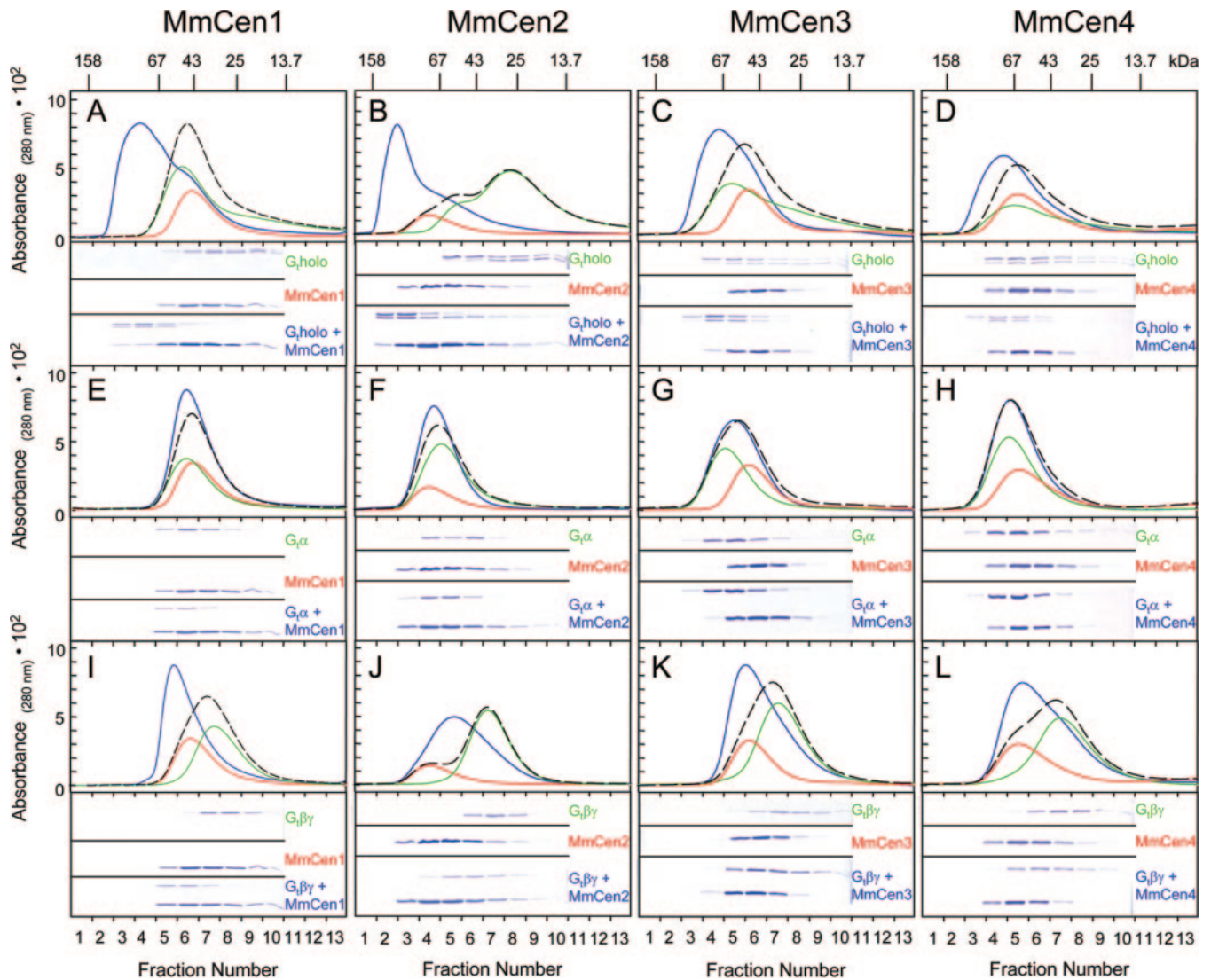


FIG. 2. **Centrin-transducin complexes analyzed by size exclusion chromatography.** The binding reaction under different conditions was analyzed by size exclusion chromatography and SDS-PAGE. *A–D* represent the interactions of G_t ,holo, *E–H* show the interactions of G_t , α , and *I–L* show the interactions of G_t , $\beta\gamma$ with the different centrin isoforms (MmCen1, MmCen2, MmCen3, and MmCen4) as indicated. Elution profiles obtained with elution buffer containing $100 \mu\text{M}$ CaCl_2 are shown for centrin isoforms alone (red), G_t or its subunits alone (green), and the mixture of centrin isoforms with G_t or its subunits (blue) in the upper panels. The dotted lines are the calculated superpositions of the respective single component profiles yielding the predicted profiles for the mixture of the two non-interacting components. SDS-PAGE analysis of the fractions of the size exclusion chromatography is shown in the lower panels. Interactions of centrin isoforms (each $10 \mu\text{g}$) with G_t ,holo ($10 \mu\text{g}$) (*A–D*), with G_t , α ($10 \mu\text{g}$) (*E–H*) and with G_t , $\beta\gamma$ ($10 \mu\text{g}$) (*I–L*) in the presence of $100 \mu\text{M}$ CaCl_2 are shown. Note that 1) the lower amplitude of the MmCen2 peak absorption compared with the other centrin isoforms is due to the fact that only one aromatic amino acid is present in this molecule and 2) G_t ,holo elutes at an apparently lower molecular weight compared with its subunits (15).

Size Exclusion Chromatography—To further validate our pull-down results, binding of purified G_t ,holo and its subunits (G_t , α and G_t , $\beta\gamma$) to the recombinant mouse centrin isoforms (MmCen1 to MmCen4) was investigated by size exclusion chromatography and SDS-PAGE/colorimetry. The elution profiles in Fig. 2, *A–D* demonstrated the presence of Ca^{2+} -dependent complexes between the G_t ,holo and all recombinant centrin isoform polypeptides by a shift of the elution peaks to higher molecular weights. The peaks were compared with a theoretical peak (black dotted line) calculated for the superposition of the single component profiles. The transducin subunits (G_t , α and G_t , $\beta\gamma$) interacted with the centrin isoforms (MmCen2 to MmCen4) in the same different Ca^{2+} -dependent manner as demonstrated previously with MmCen1 (Fig. 2, *E–L*, and Pulvermüller *et al.* (15)): the mixture of G_t , α in its inactive, GDP-bound form and all tested centrin isoforms revealed no significant shift of the elution peak as compared with the calculated trace (Fig. 2, *E–H*). Compared with G_t , α , the $\beta\gamma$

subunit shows the shift to higher molecular weight characteristic for complex formation in all samples with the different centrin isoforms (Fig. 2, *I–L*). In the presence of 1 mM EGTA (*i.e.* absence of free Ca^{2+}), no interaction of centrin isoforms were found with G_t ,holo or any of the subunits (data not shown). The SDS-PAGE patterns in the lower part of each figure yield the additional information that for all isoforms the G_t , α subunits and the G_t , $\beta\gamma$ complex are present in the complex with centrin, although G_t , α alone does not interact (Fig. 2, compare *A–D* with *E–H*). Thus, G_t can bind to the centrins in a Ca^{2+} -dependent manner as an isolated G_t , $\beta\gamma$ heterodimer or as the heterotrimeric G-protein via G_t , $\beta\gamma$.

Kinetic Light-scattering Experiments—To elaborate the interaction between the centrin isoforms with transducin in a more quantitative way, kinetic light-scattering experiments were performed. Light-scattering binding signals provide a quantitative assay of stable complex formation between transducin and Rh^* in the absence of GTP and can be readily

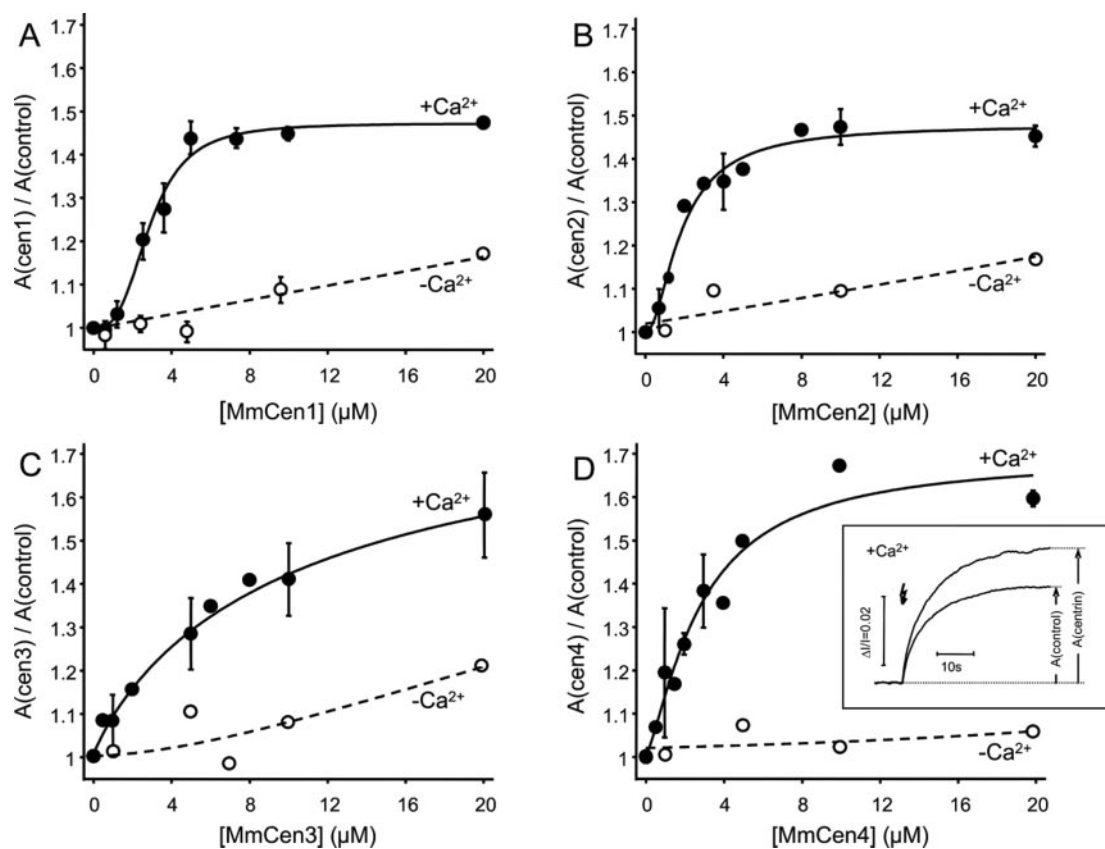


FIG. 3. Effect of centrin isoforms on the G_t binding signal analyzed by kinetic light scattering. Shown is the dependence of the amplitude of flash-induced kinetic light-scattering G_t binding signals on MmCen1 (A), MmCen2 (B), MmCen3 (C), and MmCen4 (D), respectively. In all traces the centrin isoform-dependent enhancement of the G_t binding signals (A(cen1–4)) is normalized to the amplitude of the G_t binding signal without added centrin (control), in the presence of $100 \mu\text{M}$ CaCl_2 (filled circles), or in the presence of 1 mM EGTA (open circles). Data points were fitted using the Hill equation with the parameters shown in Table I. The inset in D shows exemplarily kinetic light-scattering binding signals ($0.5 \mu\text{M}$ G_t , $3 \mu\text{M}$ rhodopsin) without and with MmCen1 ($10 \mu\text{M}$). Measurement conditions were as described under “Experimental Procedures.” The error bars display the S.D. for $n = 3$.

assayed by the transition of soluble G_t ($G_{t,\text{sol}}$) to the membrane (40, 41). Moreover, this assay is applicable to any soluble protein that interacts with Rh^* (40) and can be used as a tool to analyze changes in the amount/or molecular weight of transducin when it interacts with centrin isoforms. Addition of all recombinant mouse centrin isoforms (MmCen1 to MmCen4) resulted in an amplitude increase of the binding signal in a Ca^{2+} -dependent manner (an example is given in the inset of Fig. 3D). The increase of amplitude was significantly lower or was even not observed in the absence of free Ca^{2+} (1 mM EGTA) for all tested centrin isoforms. Titrations of the light-scattering G_t binding signals with the different centrin isoforms are shown in Fig. 3. The analysis of the titration curves of MmCen1, MmCen2, and MmCen4 revealed in the presence of Ca^{2+} that the effective concentrations of half-maximal binding (EC_{50}) are in the range of 1.8 – $2.9 \mu\text{M}$ (Table I and Fig. 3, A, B, and D). In contrast, the EC_{50} for MmCen3 was about 5 times higher than for the other centrin isoforms (Table I and Fig. 3C). This difference indicates a significant lower affinity between MmCen3 and the transducin holoprotein. In addition to the lower affinity, the titration curve of the MmCen3-transducin interaction is consistent with a model in which each G_t holoprotein binds a monomer of MmCen3 (calculated with Hill coefficient $n \leq 1$, see Table I and Fig. 3C) in contrast to the other isoforms, which most probably bind to the G-protein as homooligomers ($n \geq 1$, Table I and Fig. 3, A, B, and D).

Expression of Centrin Isoforms in Photoreceptor Cells—To evaluate the relevance of transducin binding to the centrin isoforms in photoreceptor cell function, we analyzed the expres-

TABLE I
Influence of centrin isoform concentration on calcium-dependent enhancement of the G_t binding signals probed by kinetic light scattering

Centrin isoform	Calculated fit parameter using the Hill equation ^a		
	A^b	n^c	EC_{50}^d
MmCen1	0.47 ± 0.02	3.0 ± 0.6	2.9 ± 0.2
MmCen2	0.48 ± 0.02	1.6 ± 0.4	1.8 ± 0.2
MmCen3	0.87 ± 0.37	0.8 ± 0.3	11.1 ± 10.8
MmCen4	0.69 ± 0.08	1.4 ± 0.3	2.8 ± 0.7

^a $f = (A \cdot [\text{MmCen}]^n) / ([\text{MmCen}]^n + \text{EC}_{50}^n) + 1$.

^b Maximum MmCen-dependent enhancement of the G_t binding signal.

^c Hill coefficient.

^d Effective concentrations of half-maximal binding in μM .

sion of the four centrin isoforms in the mouse retina. To address the question which of the four known centrin isoforms are expressed in the mammalian retina we first performed RT-PCR. Total RNA was extracted from isolated mouse or rat retinas, and after reverse transcription centrin cDNAs were amplified by PCR using centrin isoform-specific primer sets. Subsequently the identities of the amplified PCR products were confirmed by DNA sequencing. The present RT-PCR analysis revealed co-expression of all four centrin isoform mRNA in the adult mouse (Fig. 4) and rat retina (data not shown).

To access protein expression of the four centrin isoforms, we generated polyclonal antibodies against the recombinant centrins. The specificity of the affinity purified anti-centrin antibodies was first validated by Western blots analysis of the four

centrin polypeptides previously used as antigens for immunization. All centrin antibodies detected their centrin isoform and also cross-reacted with one (pMmC3) or more of the complementary other three centrin isoforms (Fig. 5, A–D, left panel). Since centrin isoforms are very closely related (12, 16) and the cross-reactivities between antibodies generated against centrins with other centrin family members were frequently reported in previous studies (e.g. Refs. 14, 16, and 47), these results were not surprising. To minimize or even avoid these cross-reactivities, we preadsorbed antibodies raised against a specific centrin isoform with the polypeptides of the three other centrin isoforms prior to our expression analyses. Following this approach, we were able to discriminate between the proteins of all four centrin isoforms (Fig. 5, A–D, right panel). Preadsorption of the antibodies pMmC1 to pMmC4 with

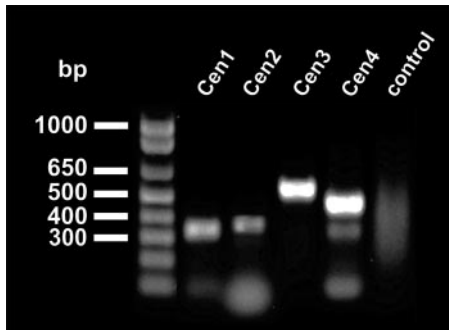


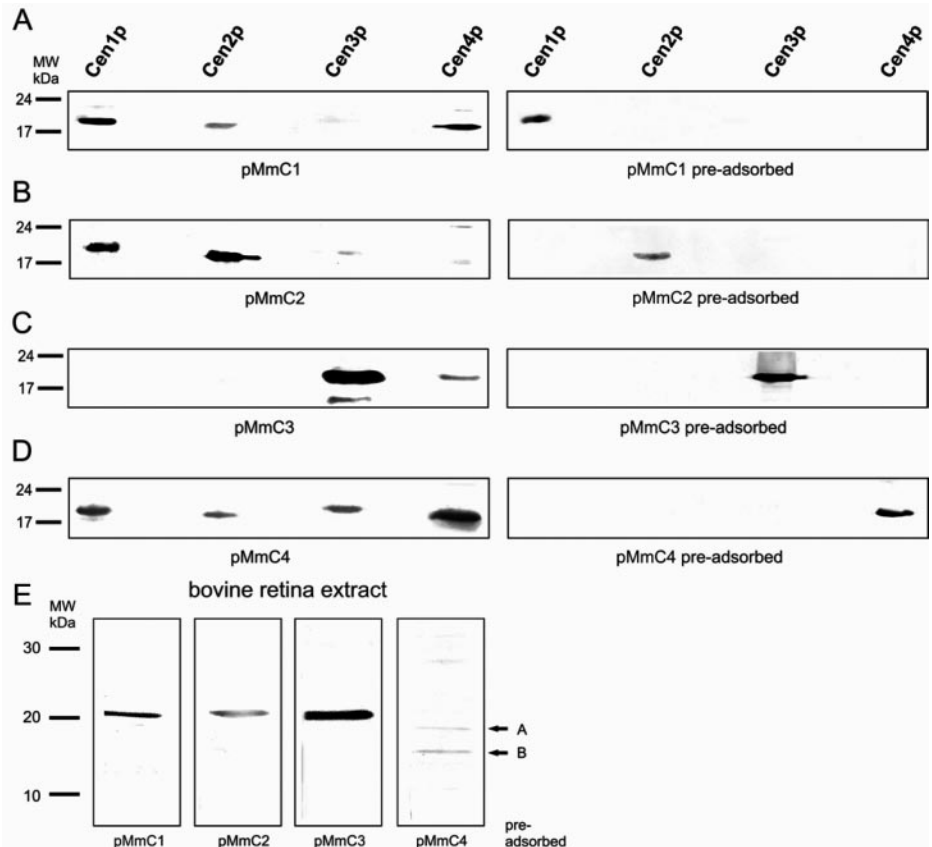
FIG. 4. Expression analysis of centrin isoforms in mouse retina by RT-PCR. Mouse centrin-specific primer sets were used to amplify different constructs of centrin isoforms. Total RNA used for all RT-PCR experiments was treated with DNase I to degrade genomic DNA. Control PCR (*control*) was conducted with DNase I-treated RNA lacking reverse transcriptase to demonstrate that no genomic DNA is amplified. All four centrin isoforms (MmCen1 to MmCen4) are expressed in the mouse retina.

the appropriate recombinant centrin proteins abolished cross-reactivity with any nonspecific centrin isoform. Subsequent Western blot analyses of proteins extracted from bovine and mouse retinas with the preadsorbed anti-centrin antibodies revealed that the proteins of all four centrin isoforms (Cen1p to Cen4p) were expressed in bovine (Fig. 5E) and mouse retinas (data not shown).

Subcellular Localization of the Complex Partners Transducin and Centrin Isoforms in Photoreceptor Cells—We studied subcellular distribution of transducin in light- and dark-adapted retinas of mice. Previous immunofluorescence studies have shown that G_t is predominantly found in the photoreceptor outer segments in dark-adapted retinas, while after light adaptation G_t moves into the inner segment of photoreceptor cells (e.g. Refs. 6, 10, and 15). The present silver-enhanced immunogold labeling confirmed in principle these overall distributions under both illumination conditions shown by indirect immunofluorescence (Fig. 6). Nevertheless the resolution of immunoelectron microscopy revealed that during light adaptation G_t accumulated in the connecting cilium of photoreceptor cells (Fig. 6A). In contrast, minor G_t labeling was present in the cilium of dark-adapted cells (Fig. 6B). In dark-adapted rods in the absence of G_t molecules in the inner segment cytoplasm, G-protein staining was also obvious in the centriole of the basal bodies localized at the base of the photoreceptor cilium (Fig. 6B).

Now we addressed the subcellular localization of the centrin isoforms in retinal photoreceptor cells. Although in previous immunocytochemical studies the centrin antibodies used were not always isoform-specific, centrin isoforms 1, 3, and 4 were suggested to localize in cilia or their basal bodies, respectively (12, 14, 27, 47). To prove the differential expression of centrin isoforms, immunocytochemical experiments with the preadsorbed antibodies pMmC1 to pMmC4 were performed in retinal cryosections. Untreated affinity-purified antibodies pMmC1 to

FIG. 5. Validation of centrin isoform antibody specificity and expression analysis of bovine retina by Western blots. Affinity-purified antibodies raised against centrin isoforms (pMmC1 to pMmC4) cross-react with recombinant centrin isoforms (Cen1p to Cen4p) in Western blots (A–D, left panels). These cross-reactivities were abolished by preadsorption of centrin pMmC antibodies with recombinant centrin polypeptides (see “Experimental Procedures”) (A–D, right panels). In Western blot analysis of bovine retinal extract with preadsorbed antibodies pMmC1, pMmC2, and pMmC3 single specific bands at 20 kDa, the molecular mass of the Cen1, Cen2, and Cen3, were detected (E). With preadsorbed pMmC4 two faint bands at about 15 (arrow B) and 19 (arrow A) kDa were recognized; these bands represent bovine Cen4 and a shorter splice variant of Cen4 identified previously in other mammalian species (27).



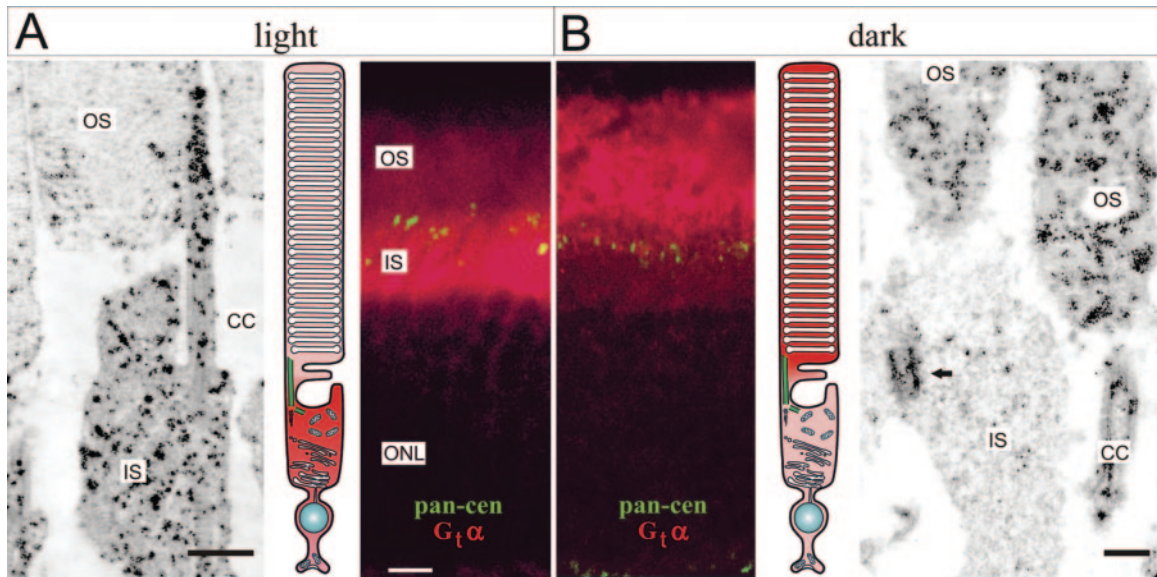


FIG. 6. **Subcellular localization of transducin and centrin in mouse retinas.** *A* and *B*, immunolocalization of G_t in light- and dark-adapted mouse photoreceptor cells via indirect green immunofluorescence (*A*, right; *B*, left) and silver-enhanced immunogold electron microscopy (*A*, left; *B*, right). *A*, after light adaptation, G_t is predominantly localized in the inner segment (IS) and the perikaryon containing the nucleus in the outer nuclear layer (ONL) down to the synaptic terminal in the outer plexiform layer (OPL). Only minor anti- G_t immunolabeling is present in the outer segment (OS). Intense silver-enhanced gold particles are present in the inner segment and accumulate in the connecting cilium (CC) linking the inner segment and outer segment. *B*, in dark-adapted photoreceptor cells G_t is predominantly localized in the outer segment. The connecting cilium is less intensely stained. In the inner segment intense labeling is restricted to the centriole of the basal body indicated by the arrow. Red double immunofluorescence of the pancentrin (pan-cen) monoclonal antibody (clone 20H5), which detects all four centrin isoforms, is present in the connecting cilium. Bars, 0.5 μm (*A*, left), 10 μm (*A*, right; *B*, left), and 0.3 μm (*B*, right).

pMmC4 reacted in addition to the connecting cilium with basal bodies and centrosomes (data not shown). In contrast, indirect immunofluorescence of pMmC1 preadsorbed with the recombinant centrin isoforms 2–4 was only present in the connecting cilium of photoreceptor cells (Fig. 7, *A* and *A'*). Thus, Cen1p expression in the retina was restricted to the connecting cilium. Indirect immunofluorescence of preadsorbed antibodies pMmC2 and pMmC3 revealed the localization of Cen2p and Cen3p in the basal body complex as well as in the connecting cilium (Fig. 7, *B* and *C* and *B'* and *C'*). In contrast, labeling with the preadsorbed pMmC4 antibody showed no ciliary staining but a basal body labeling (Fig. 7, *D* and *D'*). The ciliary localization of MmCen3 was confirmed by immunoelectron microscopic analysis with the preadsorbed pMmC3 antibody (Fig. 8*A*). In the connecting cilium, MmCen3 was localized at the inner surface of the axonemal microtubule doublets in exactly the same ciliary subdomain where we have previously found the co-localization of MmCen1/MmCen2 with transducin (15). Our present immunocytochemical studies further indicated the localization of the centrin proteins MmCen2 and MmCen3 in centrosomes of non-photoreceptor retinal cells, whereas MmCen1 and MmCen4 were not detectable there (Fig. 7, *A–D* and *A'–D'*). The differential localization of the centrin isoforms in mammalian photoreceptor cells and in non-specialized cells is summarized in the diagrams shown in Fig. 8, *B* and *C*.

DISCUSSION

This study was designed to analyze the interaction of transducin G_t , the heterotrimeric G-protein of the visual signal transduction cascade, with all four known mammalian centrin isoforms. We have demonstrated previously that the centrin isoform 1 binds with high affinity and specificity to G_t in a strictly Ca^{2+} -dependent manner (15, 16). Here we show that all four centrin isoforms are differentially expressed in mammalian photoreceptor cells and interact with transducin.

The present protein-protein interaction experiments demonstrate transducin binding to all four centrin isoforms. Centrin-GST pull-down assays and size exclusion chromatography re-

veal that the undissociable $G_t\beta\gamma$ dimer interacts with all centrin isoforms as an isolated heterodimer or within the heterotrimeric G_t holo. As demonstrated for centrin 1 by blot overlay assays in our initial studies all centrins interact via the $G_t\beta\gamma$ dimer of transducin (15, 16). Furthermore our protein-protein interaction assays show that the assembly of all centrin-transducin complexes is strictly dependent on Ca^{2+} . Previous biophysical analyses of centrins have indicated that the binding of Ca^{2+} via their EF-hands induces conformational changes of the molecules resulting in activation of centrins (18, 27, 48, 49). In diverse unicellular green algae, Ca^{2+} -activated centrins are responsible for the formation and contraction of centrin-containing nanofibers (17, 18). Although a recent study showed Ca^{2+} -independent binding of centrin to a target protein (50), in most cases the activation of centrins by Ca^{2+} is necessary for the interaction with their binding partners (16, 18). In the yeast *Saccharomyces cerevisiae*, Ca^{2+} facilitates binding of Cdc31p, the yeast centrin homologue, and of the human centrin isoforms 1 and 2 to Kar1p, which is necessary for division of the yeast cell (48, 51, 52). In our previous centrin blot overlay assays, the binding of recombinant MmCen1 to all detected interacting proteins was Ca^{2+} -dependent (15, 16). Here we show that not only the binding of centrin 1 to transducin but also of the other three centrin isoforms is triggered by Ca^{2+} .

Although all centrin isoforms interact with the $G_t\beta\gamma$ in a Ca^{2+} -dependent manner, we observed remarkable differences between the binding capacity of the centrin isoforms in particular between the isoform 3 and the other three isoforms. Our kinetic light-scattering experiments revealed that centrin 3 binds with a 5 times lower affinity to $G_t\beta\gamma$ (EC_{50} is 5 times higher) than the centrin isoforms 1, 2, and 4. However, the EC_{50} for centrin 3 binding is at least 2–3 times higher than the EC_{50} of calmodulin, previously used in a control experiment as a well known EF-hand Ca^{2+} -binding protein that is related to centrin protein family members (15). Furthermore the comparison of the obtained Hill coefficient suggested that the centrins 1, 2, and 4 interact with $G_t\beta\gamma$ as oligomers, while the centrin

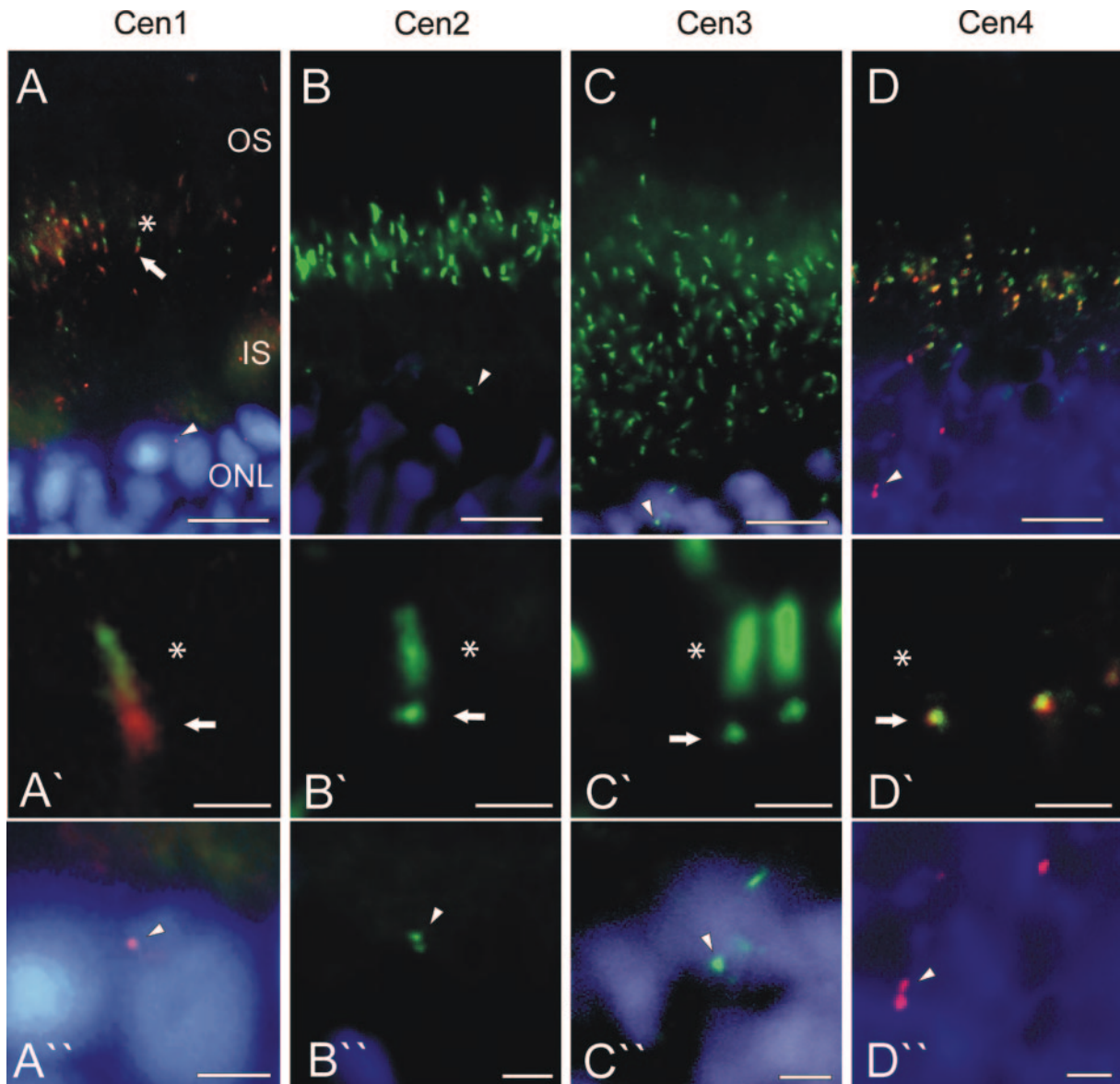


FIG. 7. **Subcellular localization of centrin isoforms in the mouse retina.** *A–D*, immunofluorescence labeling of the four centrin isoforms (Cen1 to Cen4) in longitudinal cryosections through the photoreceptor layer of mouse retinas using preadsorbed anti-centrin antibodies (green). Nuclei in the outer nuclear layer (ONL) were counterstained by 4,6-diamidino-2-phenylindole (DAPI) (blue). In *A–A'* and *D–D'* centrosomes of basal bodies and centrosomes are additionally triple stained with antibodies against γ -tubulin (red). *A–D*, in retinal photoreceptor cells, Cen1 to Cen4 are localized at the joint between inner segments (IS) and outer segments (OS). *A'–D'*, higher magnification of the immunofluorescence of the centrosomes of the photoreceptor connecting cilium (asterisk) and its basal body (arrow). *A'–D'*, higher magnification of the immunofluorescence of the centrosomes of Müller glia cells in the apical part of the outer nuclear layer. *A–A''*, indirect immunofluorescence of preadsorbed pMmC1 (green) and of anti- γ -tubulin (red). Preadsorbed pMmC1 exclusively stains the connecting cilium, which appears as a green strip (asterisk in *A'*) but not the basal body (arrow in *A'*) or the centrosomes (arrowhead in *A'*), which are marked by anti- γ -tubulin staining (arrowhead). *B–B''* and *C–C''*, indirect immunofluorescence of preadsorbed pMmC2 and pMmC3, respectively (green). Preadsorbed pMmC2 and pMmC3 stain connecting cilia (asterisks in *B'* and *C'*), the basal bodies (arrows in *B'* and *C'*), and the centrosomes (arrowheads in *B''* and *C''*). Preadsorbed pMmC4 does not stain the connecting cilium (asterisk in *D'*) but exclusively labels basal bodies (arrow in *D'*) but not the centrosomes (arrowhead in *D''*), which are marked by anti- γ -tubulin staining (arrowhead, red dots). Bars, 7.5 μ m (*A–D*), 1 μ m (*A'–D'*), and 1.9 μ m (*A'–D''*).

isoform 3 binds as a monomer in these assays. These findings confirm the ability of oligomerization, even of polymerization, of centrins previously demonstrated (48). In green algae, centrins are the major component of the contractile fibers of ciliary rootlets (19, 53). *In vitro* studies with purified centrins indicate that centrins can polymerize to large polymeric structures induced by slowly increasing the Ca^{2+} concentration (48). Future studies will be necessary to prove whether the centrin isoforms, found to co-localize in subcellular domains of photoreceptor cells, may also form heteromers.

In our initial studies, we discussed that the Ca^{2+} -induced assembly of a G-protein-centrin complex regulates the ciliary G-protein translocation in retinal photoreceptor cells (12, 15,

16). The accumulation of G_t observed in the present study in the ciliary domain of rod photoreceptor cells after light adaptation strongly suggests that the G_t -centrin complex is induced by light. In the connecting cilium previous quantification of silver-enhanced immunogold labeling demonstrated the co-localization of centrins with G_t at the inner surface of the axonemal microtubule doublets, a specific ciliary subdomain (12, 15). The present immunoelectron microscopic analysis further supports the hypothesis that centrin- G_t complexes assemble in the connecting cilium. As a consequence of the formation of this complex, the mobility of G_t through the slender cilium should decrease (barrier hypothesis discussed in Wolfrum *et al.* (16)) representing the foundation for the accumulation of G_t in the

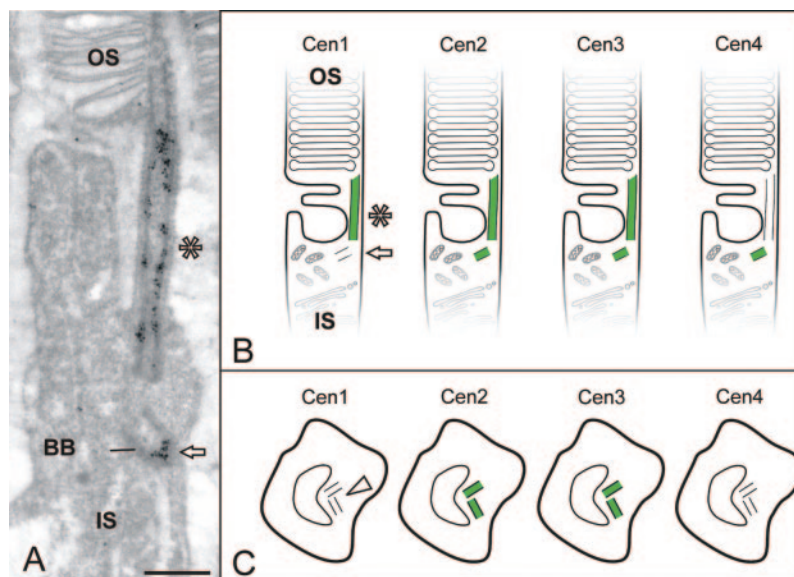


FIG. 8. Immunoelectron microscopic localization of centrin 3 in a mouse photoreceptor cell and schematic illustrations of the centrin isoform localization in photoreceptor cells and non-photoreceptor cells. A, longitudinal ultrathin section through part of mouse rod photoreceptor cell silver-enhanced immunogold labeled by preadsorbed pMmC3. Cen3 is localized in the connecting cilium (asterisk) at the inner surface of the axonemal microtubule pairs and in the centriole of the basal body (BB, arrow). Bar, 0.5 μ m. B, schematic illustration of the differential localization of the four distinct centrin isoforms in specialized vertebrate photoreceptor cells. Cen1, Cen2, and Cen3 are localized in the connecting cilium (asterisk). Cen2 and Cen3 are additionally present in the basal body (arrow). Cen4 is restricted to the basal body (arrow). C, schematic illustration of the differential localization of the four centrin isoforms in non-specialized eukaryotic cells. Cen2 and Cen3 are localized in centrioles of centrosomes, while Cen1 and Cen4 are not associated with centrosomes (arrowhead). IS, inner segment; OS, outer segment.

ciliary compartment of rod photoreceptor cells. In the connecting cilium, the assembly of the centrin-G_t complex is modulated by light and the ciliary free Ca²⁺ concentration. Changes of free Ca²⁺ in the photoreceptor within the operating (single quantum detective) range of the rod have been well studied (4). In rod operating range, a dramatic Ca²⁺ drop occurs in the outer segment after light activation of the visual cascade. However, recently a Ca²⁺ increase was observed in rod photoreceptor cells in bright light and rod-saturated conditions (54) that might be the source of Ca²⁺ for the induction of centrin/G-protein binding in the cilium.

Which centrin of the four closely related isoforms is responsible for the interaction with transducin in mammalian rods? This study has demonstrated mRNA and protein expression of four centrin isoforms in the mammalian retina, and investigations of others have found that centrin is expressed in different cellular systems (14, 27, 47). Here we show for the first time co-expression of all four centrin species in one and the same cell type. In retinal photoreceptor cells, each of the four centrin isoforms is present and should have the potential to participate in the regulation of transducin translocation through the photoreceptor cilium. The isoform-specific immunolabelings also reveal differential subcellular localizations of the isoforms in the photoreceptors. Only a subset of centrin isoforms, namely the isoforms 1, 2, and 3, are localized in the connecting cilium of photoreceptor cells. In contrast, centrin 4 is exclusively localized in the basal body at the base of the connecting cilium, leaving centrin isoforms 1, 2, and 3 as potential regulators of transducin translocation. Because centrin 3 has much lower affinity to transducin than the three other centrin isoforms, centrin 1 and 2 remain as the predominant candidates for Ca²⁺-dependent regulation of transducin translocation.

As already mentioned centrin is not only concentrated in the connecting cilium of rod cells but are also present at the centrioles of centrosomes and basal bodies (e.g. Figs. 7 and 8). Might centrin in non-ciliary localizations also interact with heterotrimeric G-proteins? Interestingly there is growing evi-

dence for functions of heterotrimeric G-proteins at centrioles present in centrosomes and spindle poles. In recent years G-protein signaling independent of membrane-integral G-protein-coupled receptors has been the focus of intensive research (for reviews, see Refs. 55–57). In embryos of *Drosophila melanogaster* and *Caenorhabditis elegans* subunits of heterotrimeric G-proteins act as effectors in the organization of asymmetric spindles (56, 57). The mitotic spindles are organized at spindle poles, which originate from centriole duplication in the G₁ phase of mitosis. Recent “knock-down” studies with small interfering RNA revealed that in human cultured cells centrin 2 is required for centriole duplication (31). In photoreceptor cells, the centrin isoforms 2, 3, and 4 are also concentrated at the centrioles. The present immunoelectron microscopy revealed that heterotrimeric G-proteins co-localize with the three centrin isoforms at photoreceptor centrioles, and upon a local increase of free Ca²⁺ centrin-G-protein complexes most probably also assemble there. These findings further support the hypothesis that centrin might be the molecular linkers between G-protein signaling and the function of spindle poles, centrosomes, and basal bodies in organizing cellular processes.

Acknowledgments—We are most grateful to J. L. Salisbury (Mayo Foundation, Rochester, MN) for kindly supplying monoclonal centrin antibodies. We thank K. Lotz, E. Sehn, G. Stern-Schneider, and K. Kubicki (University of Mainz, Mainz, Germany) and I. Semjonow and J. Engelmann (Charité, Berlin, Germany) for skillful technical assistance. We also thank M. Heck for helpful comments on the manuscript.

REFERENCES

- Pugh, E. N., Jr., and Lamb, T. (2000) in *Molecular Mechanism in Visual Transduction* (Stavenga, D. G., DeGrip, W. J., and Pugh, E. N., Jr., eds) Vol. 3, pp. 183–255, Elsevier Science Publishers B.V., Amsterdam
- Okada, T., Ernst, O. P., Palczewski, K., and Hofmann, K. P. (2001) *Trends Biochem. Sci.* **26**, 318–324
- Heck, M., and Hofmann, K. P. (1993) *Biochemistry* **32**, 8220–8227
- Molday, R. S., and Kaupp, U. B. (2000) in *Molecular Mechanism in Visual Transduction* (Stavenga, D. G., DeGrip, W. J., and Pugh, E. N., Jr., eds) Vol. 3, pp. 143–182, Elsevier Science Publishers B.V., Amsterdam
- Palczewski, K., Polans, A. S., Baehr, W., and Ames, J. B. (2000) *Bioessays* **22**, 337–350
- Sokolov, M., Lyubarsky, A. L., Strissel, K. J., Savchenko, A. B., Govardovskii, V. I., Pugh, E. N., and Arshavsky, V. Y. (2002) *Neuron* **34**, 95–106

7. Sokolov, M., Strissel, K. J., Leskov, I. B., Michaud, N. A., Govardovskii, V. I., and Arshavsky, V. Y. (2004) *J. Biol. Chem.* **279**, 19149–19156
8. Philp, N. J., Chang, W., and Long, K. (1987) *FEBS Lett.* **225**, 127–132
9. Brann, M. R., and Cohen, L. V. (1987) *Science* **235**, 585–587
10. Whelan, J. P., and McGinnis, J. F. (1988) *J. Neurosci. Res.* **20**, 263–270
11. Hardie, R. (2002) *Neuron* **34**, 3–5
12. Giessl, A., Trojan, P., Pulvermüller, A., and Wolfrum, U. (2004) in *Cell Biology and Related Disease of the Outer Retina* (Williams, D. S., ed) pp. 195–222. World Scientific Publishing Company Pte. Ltd., Singapore
13. Besharse, J. C., and Horst, C. J. (1990) in *Ciliary and Flagellar Membranes* (Bloodgood, R. A., ed) pp. 389–417. Plenum Press, New York
14. Wolfrum, U., and Salisbury, J. L. (1998) *Exp. Cell Res.* **242**, 10–17
15. Pulvermüller, A., Giessl, A., Heck, M., Wottrich, R., Schmitt, A., Ernst, O. P., Choe, H. W., Hofmann, K. P., and Wolfrum, U. (2002) *Mol. Cell. Biol.* **22**, 2194–2203
16. Wolfrum, U., Giessl, A., and Pulvermüller, A. (2002) *Adv. Exp. Med. Biol.* **514**, 155–178
17. Salisbury, J. L. (1995) *Curr. Opin. Cell Biol.* **7**, 39–45
18. Schiebel, E., and Bornens, M. (1995) *Trends Cell Biol.* **5**, 197–201
19. Salisbury, J. L., Baron, A., Surek, B., and Melkonian, M. (1984) *J. Cell Biol.* **99**, 962–970
20. Lee, V. D., and Huang, B. (1993) *Proc. Natl. Acad. Sci. U. S. A.* **90**, 11039–11043
21. Errabolu, R., Sanders, M. A., and Salisbury, J. L. (1994) *J. Cell Sci.* **107**, 9–16
22. Levy, Y. Y., Lai, E. Y., Remillard, S. P., Heintzelman, M. B., and Fulton, C. (1996) *Cell Motil. Cytoskelet.* **33**, 298–323
23. Madeddu, L., Klotz, C., Le Caer, J. P., and Beisson, J. (1996) *Eur. J. Biochem.* **238**, 121–128
24. Meng, T. C., Aley, S. B., Svard, S. G., Smith, M. W., Huang, B., Kim, J., and Gillin, F. D. (1996) *Mol. Biochem. Parasitol.* **79**, 103–108
25. Middendorp, S., Paoletti, A., Schiebel, E., and Bornens, M. (1997) *Proc. Natl. Acad. Sci. U. S. A.* **94**, 9141–9146
26. Wottrich, R. (1998) *Cloning and Computer-based Structural Analyses of Centrin Isoforms in the Rat (*Rattus norvegicus*)*. Diploma, Universität Karlsruhe, Karlsruhe, Germany
27. Gavet, O., Alvarez, C., Gaspar, P., and Bornens, M. (2003) *Mol. Biol. Cell* **14**, 1818–1834
28. Salisbury, J. L., Baron, A. T., and Sanders, M. A. (1988) *J. Cell Biol.* **107**, 635–641
29. Baron, A. T., Greenwood, T. M., and Salisbury, J. L. (1991) *Cell Motil. Cytoskelet.* **18**, 1–14
30. Baron, A. T., Greenwood, T. M., Bazinet, C. W., and Salisbury, J. L. (1992) *Biol. Cell* **76**, 383–388
31. Salisbury, J. L., Suino, K. M., Busby, R., and Springett, M. (2002) *Curr. Biol.* **12**, 1287–1292
32. Wolfrum, U. (1995) *Cell Motil. Cytoskelet.* **32**, 55–64
33. Hart, P. E., Poynter, G. M., Whitehead, C. M., Orth, J. D., Glantz, J. N., Busby, R. C., Barrett, S. L., and Salisbury, J. L. (2001) *Gene (Amst.)* **264**, 205–213
34. Laemmli, U. K. (1970) *Nature* **227**, 680–685
35. Papermaster, D. S. (1982) *Methods Enzymol.* **81**, 48–52
36. Smith, H. G., Jr., Stubbs, G. W., and Litman, B. J. (1975) *Exp. Eye Res.* **20**, 211–217
37. Bradford, M. M. (1976) *Anal. Biochem.* **72**, 248–254
38. Ernst, O. P., Bieri, C., Vogel, H., and Hofmann, K. P. (2000) *Methods Enzymol.* **315**, 471–489
39. Schröder, K., Pulvermüller, A., and Hofmann, K. P. (2002) *J. Biol. Chem.* **277**, 43987–43996
40. Heck, M., Pulvermüller, A., and Hofmann, K. P. (2000) *Methods Enzymol.* **315**, 329–347
41. Heck, M., and Hofmann, K. P. (2001) *J. Biol. Chem.* **276**, 10000–10009
42. Pulvermüller, A., Palczewski, K., and Hofmann, K. P. (1993) *Biochemistry* **32**, 14082–14088
43. Schmidt, M., Giessl, A., Laufs, T., Hankeln, T., Wolfrum, U., and Burmester, T. (2003) *J. Biol. Chem.* **278**, 1932–1935
44. Wolfrum, U. (1991) *Cell Tissue Res.* **266**, 231–238
45. Wolfrum, U., and Schmitt, A. (2000) *Cell Motil. Cytoskelet.* **46**, 95–107
46. Danscher, G. (1981) *Histochemistry* **71**, 81–88
47. Laoukili, J., Perret, E., Middendorp, S., Houcine, O., Guennou, C., Marano, F., Bornens, M., and Tournier, F. (2000) *J. Cell Sci.* **113**, 1355–1364
48. Wiech, H., Geier, B. M., Paschke, T., Spang, A., Grein, K., Steinkotter, J., Melkonian, M., and Schiebel, E. (1996) *J. Biol. Chem.* **271**, 22453–22461
49. Popescu, A., Miron, S., Blouquit, Y., Duchambon, P., Christova, P., and Craescu, C. T. (2003) *J. Biol. Chem.* **278**, 40252–40261
50. Kilmartin, J. V. (2003) *J. Cell Biol.* **162**, 1211–1221
51. Spang, A., Courtney, I., Grein, K., Matzner, M., and Schiebel, E. (1995) *J. Cell Biol.* **128**, 863–877
52. Middendorp, S., Kuntziger, T., Abraham, Y., Holmes, S., Bordes, N., Paintrand, M., Paoletti, A., and Bornens, M. (2000) *J. Cell Biol.* **148**, 405–416
53. Salisbury, J. L. (1989) *J. Physiol.* **25**, 201–206
54. Matthews, H. R., and Fain, G. L. (2001) *J. Physiol.* **532**, 305–321
55. Cismowski, M. J., Takesono, A., Bernard, M. L., Duzic, E., and Lanier, S. M. (2001) *Life Sci.* **68**, 2301–2308
56. Knust, E. (2001) *Cell* **107**, 125–128
57. Goldstein, B. (2003) *Curr. Biol.* **13**, R879–R880